



VIIRS-based remote sensing estimation of ground-level PM_{2.5} concentrations in Beijing–Tianjin–Hebei: A spatiotemporal statistical model



Jiansheng Wu ^{a,b}, Fei Yao ^a, Weifeng Li ^{c,d,*}, Menglin Si ^a

^a Key Laboratory for Urban Habitat Environmental Science and Technology, Shenzhen Graduate School, Peking University, Shenzhen 518055, PR China

^b Key Laboratory for Earth Surface Processes, Ministry of Education, College of Urban and Environmental Sciences, Peking University, Beijing 100871, PR China

^c Department of Urban Planning and Design, The University of Hong Kong, Hong Kong, SAR, China

^d Shenzhen Institute of Research and Innovation, The University of Hong Kong, Shenzhen 518057, PR China

ARTICLE INFO

Article history:

Received 30 November 2015

Received in revised form 18 June 2016

Accepted 9 July 2016

Available online xxxx

Keywords:

PM_{2.5}

VIIRS AOD

NO₂

Time fixed effects regression model

Geographically weighted regression

Beijing–Tianjin–Hebei

ABSTRACT

Satellite-based remote sensing data have been widely used in estimating ground-level PM_{2.5} concentrations as it can provide spatially detailed information. Most modern satellite-based PM_{2.5} estimates use statistical models that demand dense PM_{2.5} monitoring networks. As the national PM_{2.5} monitoring networks in China were not finished until the end of 2012, the research related to PM_{2.5} is relatively unsubstantial. To further improve the accuracy and application of remote sensing based estimation models for PM_{2.5} and take advantage of the newly established networks, we employed a time fixed effects regression model and geographically weighted regression model to develop a spatiotemporal statistical model that estimated ground-level PM_{2.5} concentrations in Beijing–Tianjin–Hebei. The time fixed effects regression model used the aerosol optical depth (AOD) data from the VIIRS (Visible Infrared Imaging Radiometer Suite) instrument as the major predictive variable along with several other dependent variables, including some factors uncommonly discussed in previous literature, i.e., the satellite-derived NO₂ concentrations of the previous day (NO₂_Lag) and four directional wind vectors, and estimated day-by-day ground-level PM_{2.5} surfaces. The geographically weighted regression model used the residuals from the time fixed effects regression model as the dependent variable and the AOD value as the independent variable. Through adding the estimated residuals back to previous surfaces, we obtained the final prediction maps of ground-level PM_{2.5} concentrations in Beijing–Tianjin–Hebei with a spatial resolution of 6 km × 6 km. The results were as follows. i). The spatiotemporal statistical model performed satisfactorily in that it successfully captured both the temporal and spatial variations in the PM_{2.5}–AOD relationships. The coefficient of determination (R^2), mean prediction error (MPE), and root-mean-square error (RMSE) were 0.88301, 8.1331 $\mu\text{g}/\text{m}^3$, and 13.0574 $\mu\text{g}/\text{m}^3$, respectively, during model fitting and 0.71889, 12.2712 $\mu\text{g}/\text{m}^3$, and 19.2927 $\mu\text{g}/\text{m}^3$, respectively, during model validation. ii). Incorporating the NO₂_Lag in the time fixed effects regression model significantly improved the model's performance and it played a positive role in ground-level PM_{2.5} concentrations. Replacing the simple wind speed with four directional wind vectors was helpful for the model's performance. iii). Meteorological factors and land use characteristics significantly affected the PM_{2.5}–AOD relationships. The temperature and surface relative humidity (SRH) played a positive role, whereas the rainfall, planet boundary layer height (PBLH), average relative humidity in the PBLH (RH_PBLH), four directional wind vectors, and normalized difference vegetation index (NDVI) played a negative role. iv). The prediction maps revealed that fine particle pollution in Beijing–Tianjin–Hebei is severe and the pollution pattern presents relatively strong seasonal heterogeneity and southeast–northwest spatial heterogeneity.

© 2016 Elsevier Inc. All rights reserved.

1. Introduction

As a result of rapid urban development and industrialization, air pollution has become a severe problem in China, especially fine particle

pollution. Previous studies have shown that China has become the worst region for fine particle pollution worldwide (van Donkelaar et al., 2010, 2015, 2016). Fine particles, also called PM_{2.5}, refer to those particles with aerodynamic diameters of <2.5 μm . Several adverse outcomes are associated with high levels of PM_{2.5} in the atmosphere. PM_{2.5} decreases the visibility of the atmosphere because of its extinction effects in the atmosphere (i.e., absorption and scattering), and this can hinder citizens' activities and the aesthetics of the urban landscape

* Corresponding author at: Department of Urban Planning and Design, The University of Hong Kong, Hong Kong, SAR, China.

E-mail address: wfl@hku.hk (W. Li).

(Tao et al., 2007; Liu et al., 2013). Epidemiological studies have shown that exposures to PM_{2.5} are associated with increased cardiovascular- and respiratory-related morbidity and mortality (Pope et al., 2002; Dominici et al., 2006; Pope and Dockery, 2006). Thus, the collection of accurate, temporally and spatially resolved PM_{2.5} exposure data is very important for conducting environmental epidemiologic studies and drafting appropriate air pollution control policies.

In the existing literature, two main ways for monitoring ground-level PM_{2.5} concentrations have been employed. One involves the use of ground-based monitoring networks that can provide highly accurate, time-continuous observations. However, such observations are costly and the current spatial distribution of monitoring sites is uneven; thus, good spatial coverage information for PM_{2.5} is definitely lacking (Li et al., 2005). The other monitoring method involves the use of satellite-based remote sensing data to estimate ground-level PM_{2.5}, and the most commonly used products are aerosol optical depth (AOD) products. AOD is the integral of light extinction caused by aerosol absorption and scattering in an atmospheric column, and it measures the degree to which aerosols prevent light from penetrating the atmosphere.

In recent years, the application of remote sensing data in air pollution monitoring studies has increased rapidly (Hoff and Christopher, 2009). Previous studies mainly used the MODIS (Moderate Resolution Imaging Spectroradiometer) AOD and MISR (Multiangle Imaging Spectroradiometer) AOD to estimate ground-level PM_{2.5}. However, their spatial resolutions are relatively coarse (MODIS AOD: 10 km, MISR AOD: 17.6 km), and thus, data integration can be difficult to perform with such products. Promising new results can potentially be obtained from the Visible Infrared Imaging Radiometer Suite (VIIRS) instrument on board the Suomi-National Polar-orbiting Partnership (Suomi-NPP) spacecraft, which was launched in October 2011. The VIIRS represents an expansion and improvement of Advanced Very High Resolution Radiometer (AVHRR) and MODIS technology, and it will likely lead to substantial improvements in the quality of radiation measurements, spectral measurement range, and spatial resolution (Schueler et al., 2002). Such data have great application potential for modeling ground-level air quality (Schliep et al., 2015; Wang et al., 2016). Therefore, one of the primary objectives of our study was to explore the performance of VIIRS AOD in estimating ground-level PM_{2.5} concentrations.

Many previous studies have established quantitative relationships between ground-level PM_{2.5} concentrations and satellite-derived AOD data by using statistical methods, such as simple linear models (Engel-Cox et al., 2004), multiple linear regression models (Jia et al., 2014), generalized linear regression models (Liu et al., 2005, 2007), generalized additive models (Liu et al., 2009), geographically weighted regression models (Hu et al., 2013; Ma et al., 2014; Song et al., 2014), linear mixed effects models (Li et al., 2015), two-stage models (Hu et al., 2014; Ma et al., 2016), and so forth. These models have similar structures that incorporate satellite-derived AOD as the main predictor variable and meteorological data, land use characteristics, and other factors as assistant variables. However, only a few models have simultaneously captured both the temporal and spatial variation of PM_{2.5}-AOD relationships successfully (Liu et al., 2009; Hu et al., 2014; Ma et al., 2016). For future studies, ignoring the spatiotemporal variation would not be scientifically justifiable and may cause large biases in the predictions. Therefore, the second objective of our study was to develop a spatio-temporal statistical model for estimating ground-level PM_{2.5} that will capture both the temporal and spatial variations simultaneously. The third objective of our study was to conduct empirical research in China, which is a problematic region for PM_{2.5} pollution, and we choose Beijing-Tianjin-Hebei as our study area. Lastly, among the previous studies, we found that the assistant variables that were used were slightly different and that the use of particular variables could be very meaningful for improvements in the model's performance. Therefore, the final objective of our study was to explore the contributions of some variables uncommonly discussed in previous literature for

improving the model's performance. These variables included satellite-derived NO₂ concentrations of the previous day (NO₂_Lag) and four directional wind vectors that were derived from the wind direction and speed.

To summarize, the objective of this study was to develop a spatio-temporal statistical model to estimate ground-level PM_{2.5} concentrations by using VIIRS AOD as the main predictive variable and other assistant variables including some newly introduced variables. This research represents empirical research on the country of China, and the resulting data may have implications for implementing action plans to control air pollution (Ministry of Environmental Protection of the People's Republic of China, 2013) and environmental epidemiological studies. In the following sections, we will describe the data and methods first, and then the results and discussion material are presented. The conclusions are summarized at the end of the paper.

2. Data and methods

2.1. Ground PM_{2.5} measurements

Ground PM_{2.5} measurements in Beijing-Tianjin-Hebei from January 1, 2014 to December 31, 2014 were collected from the official web site of the China Environmental Monitoring Center (CEMC) (<http://113.108.142.147:20035/emcpublish/>) and the official web site of the Beijing Municipal Environmental Monitoring Center (BJMEMC) (<http://zx.bjmemc.com.cn/>). According to the environmental protection standard of China, the ground PM_{2.5} data for China's mainland were measured by the tapered element oscillating microbalance (TEOM) method or the beta-attenuation method using appropriate calibration processes and quality controls (HJ618-2011, 2011). Data from 104 monitoring sites in Beijing-Tianjin-Hebei are included in this paper (Fig. 1).

2.2. Satellite AOD retrievals

The VIIRS is one of five instruments on board the Suomi-NPP satellite. The Suomi-NPP satellite, and therefore the VIIRS, has an 824 km sun-synchronous orbit (inclination = 98.7°) with a 1:30 pm local solar time ascending node. It achieves global coverage daily and has a repeat cycle of approximately 16 days. The VIIRS has a swath width of 3040 km with a spatial resolution of ~375 m at nadir in the Imagery (I) Bands and ~750 m at nadir in the Moderate (M) Bands. The VIIRS aerosol retrievals are performed at the M-band pixel level and produce a full set of aerosol parameters called the intermediate product (IP) including AOD at 550 nm. Through a system of quality checks, filtering, and spatial aggregation of 8 × 8 pixel IP values, the official level 2 product of the VIIRS, the environmental data record (EDR), is generated. That process enables the VIIRS to control pixel growth towards the edge of a scan such that the pixel sizes are comparable to nadir. Thus, the spatial resolution of the VIIRS EDR data is 6 km × 6 km (Jackson et al., 2013). In this study, we used the EDR to collect the AOD data from January 1, 2014 to December 31, 2014 in Beijing-Tianjin-Hebei; these data can be downloaded from the comprehensive larger array-data stewardship system (<http://www.class.ngdc.noaa.gov/saa/products/welcome>). Along with the AOD data, four quality flags that determine the accuracy of the AOD data were downloaded. The descriptions and percentages of these four quality flags are displayed in Table 1. To minimize the influence of AOD inaccuracy, we only used the AOD data with a quality assurance confidence flag = 3; an action strongly recommended by the VIIRS aerosol team (see the latest Readme file on product maturity: http://www.nsof.class.ngdc.noaa.gov/release/data_available/npp/npp_public_data_table.htm). The spatiotemporal coverage of VIIRS AOD data after data filtering was approximately 13.18%.

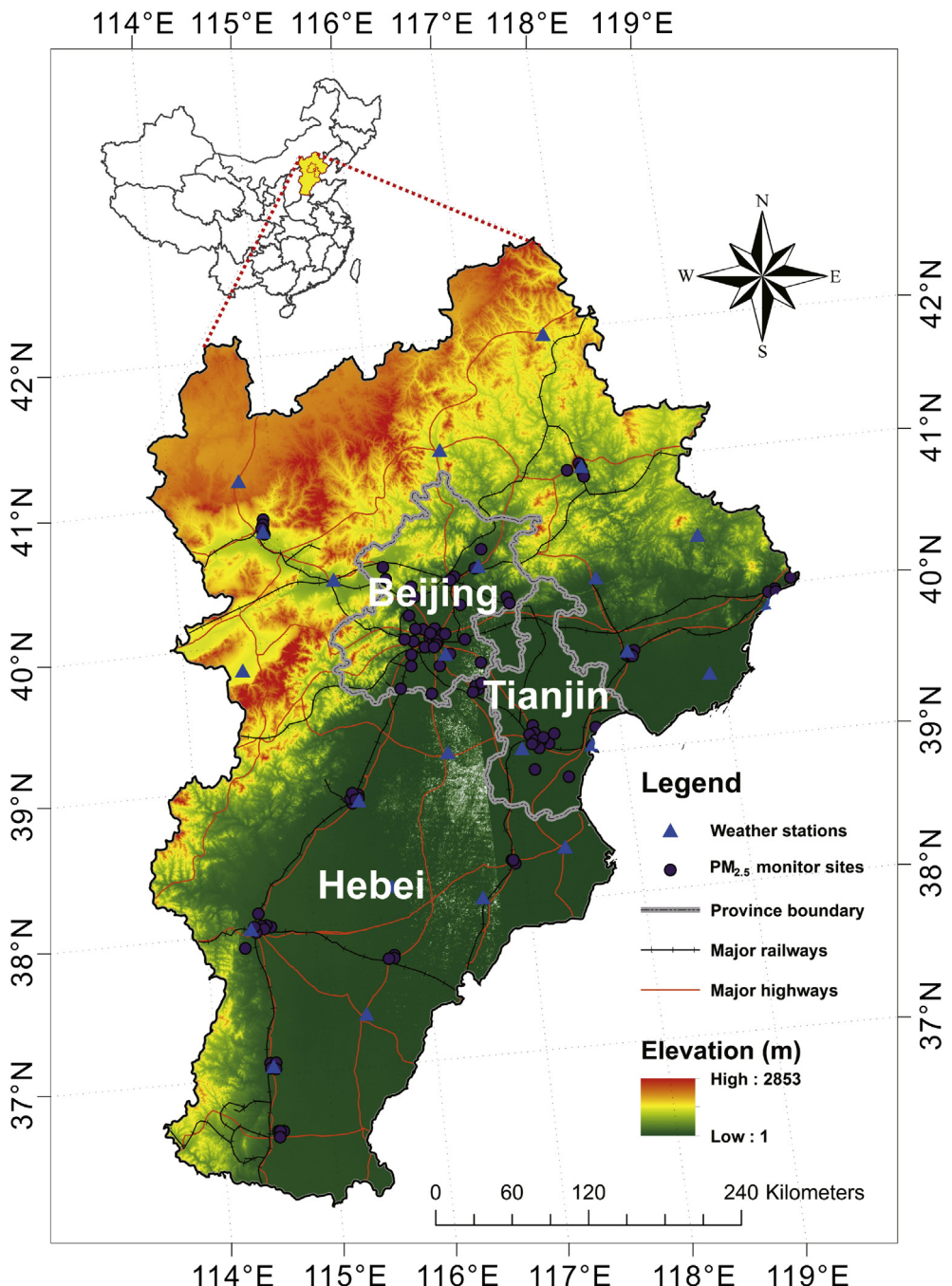


Fig. 1. Spatial distribution of PM_{2.5} monitoring sites and weather stations involved in this study.

Table 1
Descriptions and percentages of quality flags.

Flags	Quality	Descriptions	Percentage
0	Not produced	No good/degraded quality pixel retrievals Neither land or sea water dominant Ellipsoid fill in the geolocation Night scan Solar zenith angle >80°	63.07%
1	Low	Number of good/degraded quality retrievals < 16	11.88%
2	Medium	Number of good quality retrievals ≤ 16 and the number of good/degraded quality retrievals ≥ 16	11.87%
3	High	Number of good quality retrievals > 16	13.18%

2.3. Surface meteorological data and aerological data

In this study, we used both surface meteorological data and aerological data. The surface meteorological data were downloaded from the China Meteorological Data Sharing Service System (<http://www.escience.gov.cn/metdata/page/index.html>). These data included the temperature (TP), surface relative humidity (SRH), rainfall (RF), wind speed (WS), and wind direction (WD) from January 1, 2014 to December 31, 2014 in Beijing-Tianjin-Hebei; all of these data were daily averages. Data from 25 weather stations in Beijing-Tianjin-Hebei were included in this paper (Fig. 1). The aerological data were from the MERRA model reanalysis (Rienecker et al., 2011), and these data

were downloaded from the Goddard Earth Sciences Data and Information Services Center (http://disc.sci.gsfc.nasa.gov/daac-bin/FTPSubset.pl?LOOKUPID_List=MAI3CPASM). We mainly collected two kinds of aerological data, namely, the planet boundary layer height (PBLH) and the average RH in the PBLH (RH_PBLH). These data had spatial resolutions of $0.5^\circ \times 0.5^\circ$ and $1.25^\circ \times 1.25^\circ$, respectively. Corresponding to the satellite overpass time (13:30 pm local solar time), the mean value of the PBLH between 12:30 pm and 14:30 pm local solar time and the mean value of the average RH in the PBLH between 12:00 pm and 15:00 pm local solar time were extracted. Like the above-mentioned data, we collected the aerological data from January 1, 2014 to December 31, 2014 in Beijing–Tianjin–Hebei.

2.4. Satellite-derived NDVI and NO₂ data

The normalized difference vegetation index (NDVI) data with a spatial resolution of $250\text{ m} \times 250\text{ m}$ and a temporal resolution of 16 days were downloaded from the National Aeronautics and Space Administration's (NASA's) Goddard Space Flight Center (<https://ladsweb.nascom.nasa.gov/data/search.html>). The ozone monitoring instrument (OMI) sensor provided various data products including NO₂ and SO₂. We downloaded the NO₂ data (Boersma et al., 2011) from the following web site: http://www.temis.nl/airpollution/no2col/no2regioomi_v2.php. The spatial resolution of the data was $0.25^\circ \times 0.25^\circ$, and we used ground monitoring NO₂ data to evaluate the preciseness of the satellite-derived NO₂ data. The correlation coefficient between them was 0.65832 (SI, Fig. S1). We collected the data records for both of these variables from January 1, 2014 to December 31, 2014 in Beijing–Tianjin–Hebei.

2.5. Data integration

Since the original projections and spatial resolutions of the datasets varied, all the datasets were reprojected to the Albers Equal Area Conic coordinate system (Asia_North_Albers_Equal_Area_Conic in ArcGIS 10.1) before combining them. This coordinate system was chosen mainly because of its proven adaptability in the provinces and regional areas under study or in other areas that share a similar extent (Zhu et al., 2010). For all the independent variables, a nearest neighbor approach was applied. That is, for the remote sensing data including VIIRS AOD, aerological data, NDVI, and NO₂, the values of the pixel for the nearest PM_{2.5} monitoring site were extracted and assigned to the corresponding PM_{2.5} values. For the surface meteorological data, we created a network of Thiessen polygons by using weather stations, and attribute information of the polygon for the nearest PM_{2.5} monitoring site was extracted and assigned to the corresponding PM_{2.5} values. We dropped those days whose number of valid data records was less than or equal to 3, so the latter GWR equations for each day would be solvable both in model fitting and cross validation. After filtering, there were 2833 data records. The percentage of data removed was approximately 3.51%. Each data record specifically points to a certain day and a certain site. Therefore, they are time series and cross-sectional data or panel data.

2.6. Model development and validation

Since our study area was relatively large and our study period was relatively long, the relationship between PM_{2.5} and AOD was expected to vary in both space and time. To address both the spatial and temporal heterogeneity of the PM_{2.5}–AOD relationship, we developed a combined model. That is, in the first stage, we used a time fixed effects regression model to capture the temporal variation, and in the second stage, we added a geographically weighted regression model to further capture the spatial variation (Fig. 2). For the time fixed effects regression model, we only let the intercept vary with time to avoid a decrease in the model's generalization ability brought about by the model's over

complexity. The time fixed effects regression model can be expressed as follows:

$$\begin{aligned} PM_{2.5,st} = & \text{Intercept}_t + \beta_{AOD} \times AOD_{st} + \beta_{TP} \times TP_{st} + \beta_{SRH} \times SRH_{st} \\ & + \beta_{RF} \times RF_{st} + \beta_{PBLH} \times PBLH_{st} + \beta_{RH_PBLH} \times RH_PBLH_{st} \\ & + \beta_{NDVI} \times NDVI_{st} + \beta_{NO_2_Lag} \times NO_2_Lag_{st} + \beta_{TOE} \times TOE_{st} \\ & + \beta_{TOS} \times TOS_{st} + \beta_{TOW} \times TOW_{st} + \beta_{TON} \times TON_{st} + \varepsilon_{st} \end{aligned} \quad (1)$$

where $PM_{2.5,st}$ is the daily-averaged ground-level PM_{2.5} concentration ($\mu\text{g}/\text{m}^3$) at site s during day t ; Intercept _{t} is the intercept for day t ; AOD_{st} is the VIIRS AOD value (unitless) at site s during day t ; β_{AOD} is the slope for the AOD; TP_{st} is the temperature ($0.1\text{ }^\circ\text{C}$) at site s during day t ; β_{TP} is the slope for the temperature; SRH_{st} is the surface relative humidity (%) at site s during day t ; β_{SRH} is the slope for the surface relative humidity; RF_{st} is the rainfall (0.1 mm) at site s during day t ; β_{RF} is the slope for the rainfall; $PBLH_{st}$ is the planet boundary layer height (m) at site s during day t ; β_{PBLH} is the slope for PBLH; RH_PBLH_{st} is the average relative humidity in the PBLH (unitless) at site s during day t ; β_{RH_PBLH} is the slope for RH_PBLH; $NDVI_{st}$ is the normalized difference vegetation index (unitless) at site s during day t ; β_{NDVI} is the slope for NDVI; $NO_2_Lag_{st}$ is the NO₂ concentrations ($10^{15}\text{ molec}/\text{cm}^2$) at site s during day $t-1$; $\beta_{NO_2_Lag}$ is the slope for NO₂_Lag; TOE_{st} , TOS_{st} , TOW_{st} , and TON_{st} are the four directional wind vectors (0.1 m/s) at site s during day t ; and β_{TOE} , β_{TOS} , β_{TOW} , and β_{TON} are slopes for TOE, TOS, TOW, and TON (see definitions provided below) respectively. ε_{st} is the error term at site s during day t . The following points should be noted. First, given that the temporal resolution of the NDVI was 16 days, for a specific day, the NDVI that was nearest to that day was adopted. Second, when creating data records for model building, we used the NO₂_Lag as the independent variable in consideration of the lag time of chemical reactions. Third, TOE, TOS, TOW, and TON represent the west, north, east, and south wind vectors, respectively, and they were derived from the wind speed (WS) and wind direction (WD) by use of the following formulas:

$$TOE = \begin{cases} |WS \times \sin(WD)|, WD \in [0, \pi] \\ 0, WD \in [\pi, 2\pi] \end{cases} \quad (2)$$

$$TOW = \begin{cases} 0, WD \in [0, \pi] \\ |WS \times \sin(WD)|, WD \in [\pi, 2\pi] \end{cases} \quad (3)$$

$$TOS = \begin{cases} 0, WD \in [0, \frac{\pi}{2}] U(\frac{3\pi}{2}, 2\pi) \\ |WS \times \cos(WD)|, WD \in [\frac{\pi}{2}, \frac{3\pi}{2}] \end{cases} \quad (4)$$

$$TON = \begin{cases} |WS \times \cos(WD)|, WD \in [0, \frac{\pi}{2}] U(\frac{3\pi}{2}, 2\pi) \\ 0, WD \in [\frac{\pi}{2}, \frac{3\pi}{2}] \end{cases} \quad (5)$$

Eq. (1) was applied to the entire fitting dataset to generate the same slopes for all days and different intercepts for each day. Thus, the first stage time fixed effects regression model can account for the day-to-day variability in the PM_{2.5}–AOD relationship.

The residuals were obtained after the first stage. To capture the spatial variation of the PM_{2.5}–AOD relationship, we developed a geographically weighted regression (GWR) model by using the residuals as the dependent variable and the AOD values as the independent variable. Through adding residuals estimated from the GWR model to the first stage, we could capture the spatial variation of the PM_{2.5}–AOD relationship. The GWR generates a continuous surface of parameter values by taking measurements of the parameters at each local observation to denote the spatial variations of the surface (Brunsdon et al., 1996; Fotheringham et al., 1996). It should be noted that the GWR can be fitted using averaged dependent and independent variables for specific time

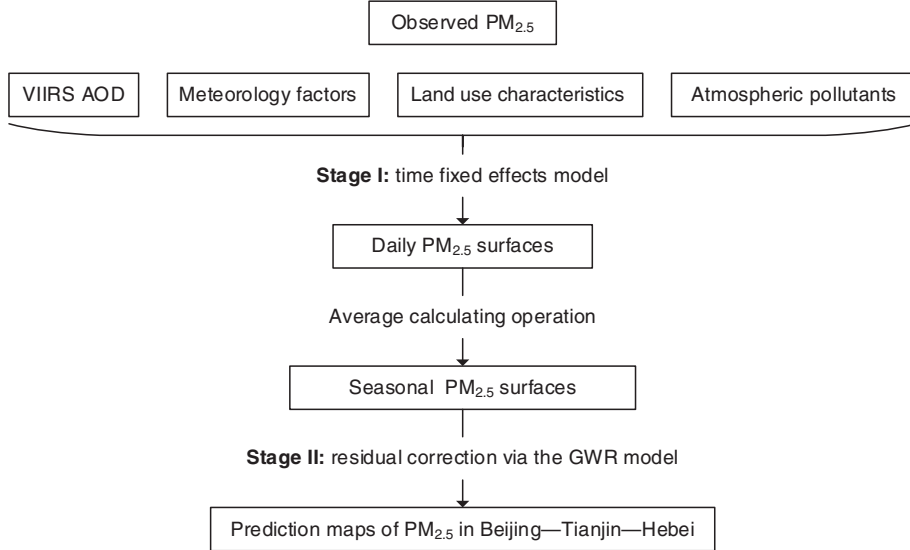


Fig. 2. Flowchart of the proposed methods.

periods, such as different seasons, or be fitted for each day separately. We tested both and found that day-by-day GWR fitting let us drop more 18 day data records and daily estimate would probably become incomparable due to the different combinations of bandwidth and bandwidth-solving algorithms, which were employed to generate as many GWR solutions as possible. Therefore, in the second stage, we fitted the GWR model by using the averaged dependent and independent variables for those days in spring, summer, autumn and winter. The GWR model structure can be expressed as follows:

$$\text{Residual}_{ss'} = \beta_{0,s} + \beta_{AOD,s} \times AOD_{ss'} + \varepsilon_{ss'} \quad (6)$$

where $\text{Residual}_{ss'}$ denotes the averaged residuals from the stage one model at site s in season s' ; $AOD_{ss'}$ is the average VIIRS AOD values at site s in season s' ; $\beta_{0,s}$ and $\beta_{AOD,s}$ denote the location-specific intercept and slope, respectively; and $\varepsilon_{ss'}$ is the error term at site s in season s' .

Previous studies have proven that parameter estimation for the GWR model is not sensitive to the kernel function, whereas this process is very sensitive to bandwidth, which specifies how the extent of the kernel should be determined (Tan, 2007). Given the uneven spatial distribution of PM_{2.5} monitoring sites, we used the adaptive bandwidth through employing the minimum AIC_c (corrected Akaike Information Criterion); thus, we obtained the best bandwidth for each monitoring site and finally built the GWR model (Fotheringham et al., 2002). The estimated residuals were added back to the estimated PM_{2.5} concentrations in the first stage, and thus, we obtained the final estimated PM_{2.5} concentrations from the combined model. We calculated the Moran's I for the residuals during both the first stage and second stage to evaluate whether the spatial variation of the PM_{2.5}-AOD relationship could be captured or not.

To assess the goodness of fit of the model, we calculated several statistical indicators between the predicted PM_{2.5} concentrations from the fitted model and the observations. These indicators included the coefficient of determination (R^2), mean prediction error (MPE), and root-mean-square error (RMSE). Potential model over-fitting may occur during model building which means models can perform better with the data used to fit the model than with the unused data. To test for this over-fitting, we conducted a 10-fold cross validation analysis. This procedure can be briefly described as follows. The entire model-fitting dataset was first randomly split into 10 subsets with about 10% of the total data records in each subset. In each round of cross validation, we selected one subset as testing samples and used the remaining nine subsets to fit the model. Then, the fitted model was used to predict the held-

out subset. In the next round, we changed the testing samples with another subset, and the training subsets were also changed synchronously. This process was repeated 10 times so as to test every subset. The agreement between the predicted and observed values was assessed with the R^2 , MPE, and RMSE values. Then, these statistics from the cross validation and model fitting procedures were compared to evaluate the degree of potential model over-fitting. It is worth noting that whereas the absolute minimum number of matched observations required to solve a GWR equation is two in order to fit an intercept and a slope, we required at least a total number of four observations per day to avoid encountering no solutions in the cross validation during stage II. Besides, similar to the model fitting, we also calculated the Moran's I for the residuals in the two stages to evaluate whether the spatial variation of the PM_{2.5}-AOD relationship could be captured or not during the cross validation.

2.7. Regression mapping

After building the models, we used the time fixed effects regression model to estimate the ground-level PM_{2.5} concentrations in the study domain where there are no PM_{2.5} observations and continuous PM_{2.5} surfaces were generated for each day. Seasonal and annual surfaces were derived from daily surfaces, and they were further corrected by using the GWR model. Thus, we obtained the final seasonal and annual surfaces that captured both temporal and spatial variations. Besides, in order to limit the concentrations to a reasonable range, predicted concentrations at the low and high ends were truncated at a certain percentage of the measured maximum/minimum values referring to some land use regression studies (Abernethy et al., 2013; Amini et al., 2014; Henderson et al., 2007; Wu et al., 2015). There was no rigorous standard applied to cutting the range down for the predicted concentrations. In general, we made assumptions similar to those described in Wu et al. (2015) and predicted concentrations were truncated at 120% of the maximum and 60% of the minimum measured values.

3. Results

3.1. Descriptive statistics

Fig. 3 illustrates the histograms and descriptive statistics for the dependent variable and all the independent variables. It shows that except for the RF, the remaining variables were approximately normally distributed (TP, SRH, NDVI, PBLH, RH_PBLH, WS) or log-normally

distributed ($\text{PM}_{2.5}$, AOD, $\text{NO}_2\text{-Lag}$). As for the wind direction, the wind from the west-south direction occurred more frequently than that from the other directions. Overall, the mean $\text{PM}_{2.5}$ concentrations for all the monitoring sites over the entire year was $92.3 \mu\text{g}/\text{m}^3$. Taking the ambient air quality standard (GB3095–2012) (Ministry of Environmental Protection of the People's Republic of China, 2012), which has been enforced since the year 2016 in China, as a reference, the annual concentration found in this study exceeded the Level 2 annual $\text{PM}_{2.5}$ standard ($35 \mu\text{g}/\text{m}^3$) by 164%. Hence, these data show the severity of the air quality problems in Beijing–Tianjin–Hebei.

3.2. Model fitting results

The slopes and first day's intercept of the time fixed effects regression model and the coefficients of the pooled regression model are shown in Table 2. The intercept differences between the rest days and first day of the time fixed effects regression model are shown in Fig. 4. In the pooled regression model, the intercept and all the independent variables were significant at the $\alpha = 0.05$ level except for the TOE, TOW, and TON. While in the time fixed effects regression model, only the TOE was not significant. Though the NDVI and $\text{NO}_2\text{-Lag}$ changed from being significant at the $\alpha = 0.05$ level to being significant at the $\alpha = 0.1$ level in the pooled regression model and the time fixed effects regression model, respectively, Fig. 4 shows that there are 104 of the newly added time dummy variables were significant at the $\alpha = 0.05$ level compared the entire 112 newly added time dummy variables; thus, the proportion of significant time dummy variables was approximately 92.86%, and given that the R^2 for the time fixed effects regression model was 0.7146 compared to just 0.4435 for the pooled regression model, use of the time fixed effects regression model was clearly advantageous. We also considered a time random effects regression model, but results from a Hausman test indicated that the time fixed effects regression model would be more reasonable to use with our dataset.

The slopes of the independent variables in the time fixed effects regression model and the coefficients of the independent variables in the pooled regression model had the same sign except for the TP (Table 2). The sign of the slopes indicated that the AOD, TP, SRH, and $\text{NO}_2\text{-Lag}$ had a positive relationship with the $\text{PM}_{2.5}$ concentrations (positive b values), whereas RF, PBLH, RH_PBLH, NDVI, and the four directional wind vectors had a negative relationship with the $\text{PM}_{2.5}$ concentrations (negative b values). This was due to several factors. The AOD values are positively correlated to the number of particles in the air, and thus, a high AOD

level means that there are high ground-level $\text{PM}_{2.5}$ concentrations as $\text{PM}_{2.5}$ is one of the main types of particles in the air. Temperature was positively correlated to ground-level $\text{PM}_{2.5}$ concentrations because high temperatures can accelerate the generation of secondary particles near the surface (Liu et al., 2007). The SRH played a positive role in increasing the ground-level $\text{PM}_{2.5}$ mainly because of its influence on water soluble components of the whole particles (Cheng et al., 2015). The $\text{NO}_2\text{-Lag}$, which represents one of the possible original sources for $\text{PM}_{2.5}$ (Zhang and Cao, 2015), may be completely or partly changed into $\text{PM}_{2.5}$ through chemical reactions after a period of time (i.e., 1 d), so its fixed slope was positive. However, we also recognized that the role of NO_2 in generating $\text{PM}_{2.5}$ was small, which can be inferred from the following two statistical validations. The magnitude ratio of AOD to $\text{NO}_2\text{-lag}$ in the time fixed effects regression model was $50.778/10.195 \approx 5$. We can roughly say that the AOD played approximately 5 times the role of NO_2 in generating $\text{PM}_{2.5}$, indicating that NO_2 was just a small contributor to $\text{PM}_{2.5}$. We see that the p-value of $\text{NO}_2\text{-Lag}$ in the time fixed effects regression model was large at 0.098, indicating NO_2 did not play a significant role. In summary, the NO_2 did contribute to the generation of $\text{PM}_{2.5}$, but the degree was small. Rainfall can wash out the particles in the air and reduce the ground-level $\text{PM}_{2.5}$ concentrations. A lower PBLH can increase the ground-level $\text{PM}_{2.5}$ concentrations by reducing vertical mixing, so its sign was negative. High RH_PBLH can increase the size and light extinction efficiencies of some particles such as ammonium sulfate and ammonium nitrate, but the $\text{PM}_{2.5}$ measurements only account for dry particle mass under controlled RH conditions ($\text{RH} = \sim 40\%$), so the same AOD value at high RH_PBLH levels represents a lower particle dry mass (lower $\text{PM}_{2.5}$ concentrations) than that at low RH_PBLH conditions (Liu et al., 2005). NDVI can reflect the variation of vegetation, which can affect ground $\text{PM}_{2.5}$ concentrations by capturing particles on plant leaf surfaces or in leaf wax (Nowak et al., 2006; Pugh et al., 2012), as a result of which, it may have some influence on $\text{PM}_{2.5}$ –AOD relationship. And that was high NDVI values are associated with lower ground-level $\text{PM}_{2.5}$ concentrations in Beijing–Tianjin–Hebei region. High wind speed can increase both horizontal and vertical mixing and therefore dilute ground-level $\text{PM}_{2.5}$ concentrations. However, it is worth noting that the TOE (wind from the western direction) was not significant, which indicates that it may have a positive relationship with ground-level $\text{PM}_{2.5}$ concentrations; this may be due to the sand dust carried with the wind, as typical sand storm phenomena occur in Beijing–Tianjin–Hebei every year. As for the individual intercept for each day, we think they measured the

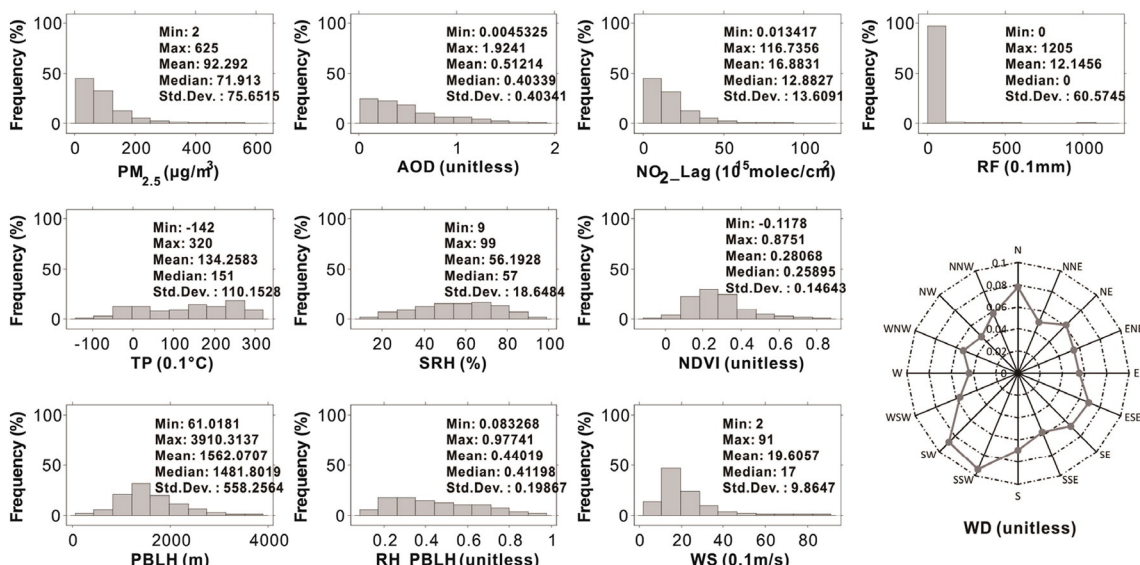


Fig. 3. Histograms and descriptive statistics for the dependent variable and all the independent variables.

Table 2

Slopes and first day's intercept of the time fixed effects regression model and the coefficients for the pooled regression model.

	Time fixed effects regression model			Pooled regression model	
	b	P-value	Magnitude ^{a)}	b	P-value
Intercept ^{b)}	40.8128	0.000		66.27389	0.000
AOD (unitless)	26.49873	0.000	50.778	43.95093	0.000
TP (0.1 °C)	0.5142278	0.000	213.919	-0.032572	0.001
SRH (%)	1.059388	0.000	82.632	0.4690842	0.000
RF (0.1 mm)	-0.0478539	0.003	-33.498	-0.0563907	0.001
PBLH (m)	-0.003909	0.004	-13.951	-0.0118985	0.000
RH_PBLH (%)	-28.16496	0.000	-21.421	-82.87771	0.000
NDVI (unitless)	-5.910207	0.051	-4.843	-9.107718	0.022
NO ₂ _Lag (10 ¹⁵ molec/cm ²)	0.1229717	0.098*	10.195	1.019493	0.000
TOE (0.1 m/s)	-0.0782302	0.267**	-3.651	-0.0632381	0.418**
TOS (0.1 m/s)	-0.4137117	0.000	-23.582	-0.4982839	0.000
TOW (0.1 m/s)	-0.2280643	0.007	-9.903	0.0964041	0.287**
TON (0.1 m/s)	-0.2151316	0.005	-8.546	-0.0604174	0.473**

* The variable is significant at the $\alpha = 0.1$ level.

** The variable is not significant.

^a Using the product of b and the corresponding variable range as the simple estimate of magnitude, which indicates what variables drive the model-estimated PM_{2.5}.

^b The intercept of the first day.

influences of those unobserved time-varying variables on the PM_{2.5}-AOD relationship. Besides, the influence of special events (e.g., APEC) on the PM_{2.5}-AOD relationship may also be measured in the individual intercepts.

Fig. 5 shows the spatial distribution of the AOD coefficients when building the GWR model between the seasonal mean residuals from the time fixed effects regression model and the seasonal mean AOD values. The uneven spatial pattern of AOD coefficients indicates that the relationship between ground-level PM_{2.5} concentrations and AOD values varies spatially. From the proportions of coefficient above and below zero in the four seasons, we concluded that we tend to underestimate ground-level PM_{2.5} in winter and spring and overestimate ground-level PM_{2.5} concentrations in summer in the first stage. Additionally, the GWR model captured this variation because the position information was embedded in the regression equation, consequently correcting the underestimation and overestimation to a certain degree.

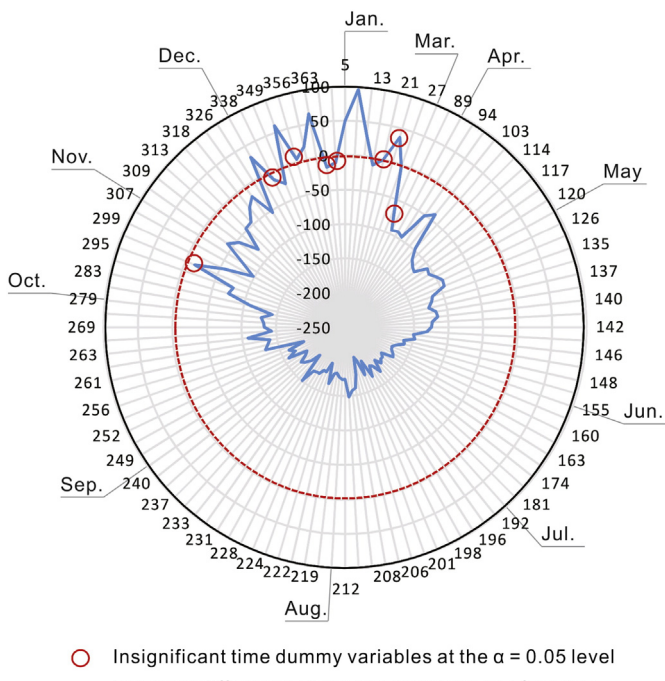


Fig. 4. Intercept differences between the rest days and first day of the time fixed effects regression model.

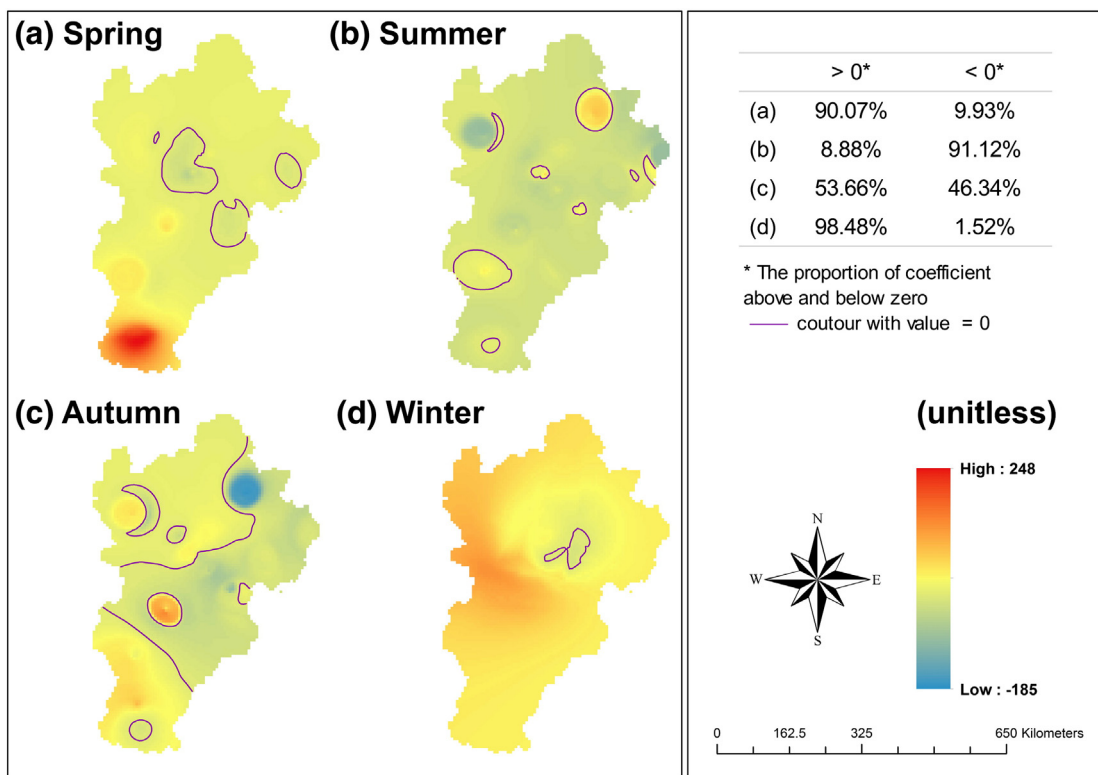
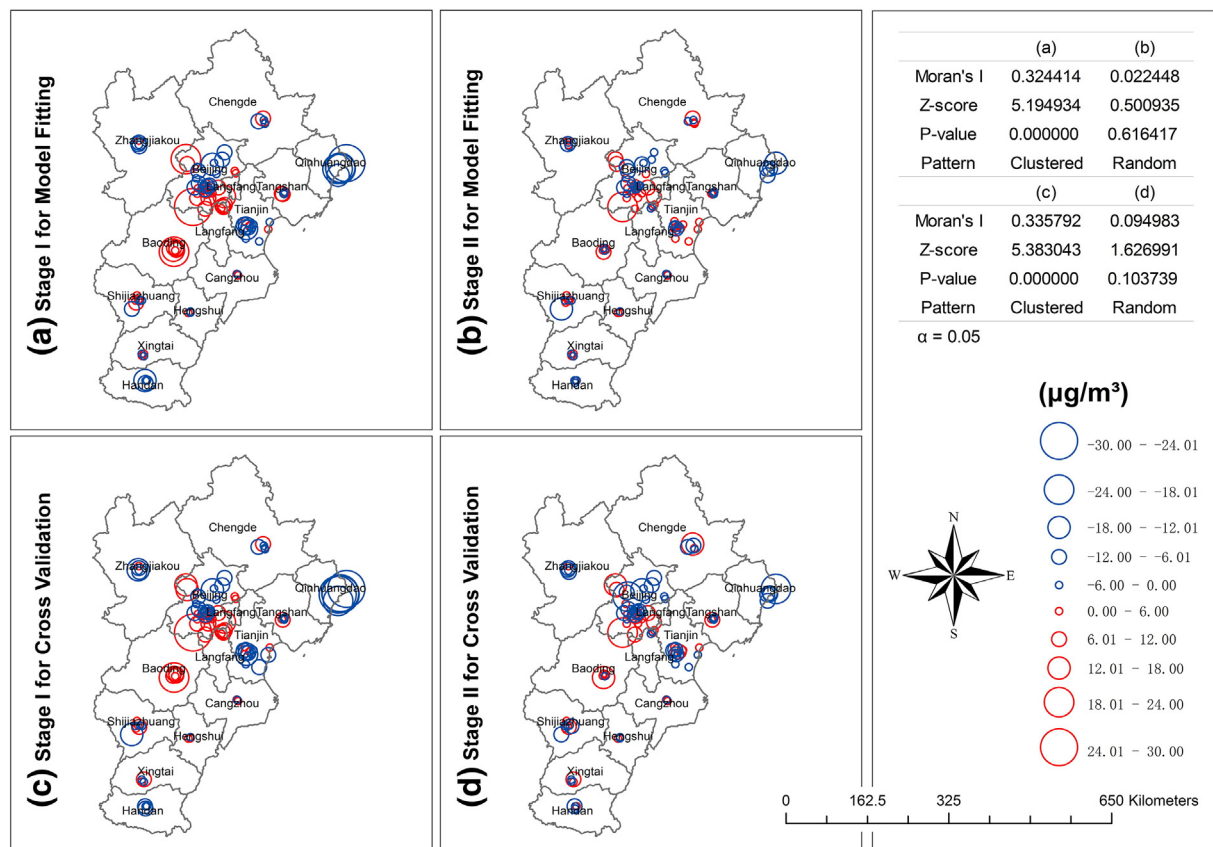
The spatially heterogeneous PM_{2.5}-AOD relationship can be demonstrated twice again in the residual spatial autocorrelation analysis and in the model validation results that are presented in the following sections.

3.3. Residual spatial autocorrelation results

Fig. 6 illustrates the residuals at each monitoring site and the corresponding Moran's I values. Subgraphs (a) and (c) show that without the GWR model, there was a trend whereby the positive residuals were intertwined with positive residuals (the locations of positive residuals were spatially near, the following cases were similar), and negative residuals were intertwined with negative residuals. The Moran's I for (a) and (c) were 0.324414 and 0.335792, respectively, and both were significant at the $\alpha = 0.05$ level, which shows that the residuals at each monitoring site were associated with positive spatial autocorrelation. Subgraphs (b) and (d) show that after application of the GWR model, there was a trend whereby the positive residuals were intertwined with the negative residuals. Moreover, a residual spatial autocorrelation test showed that no systematic pattern could be observed in subgraphs (b) and (d). Fig. 6 once again proves that the GWR model captured the spatial variation in the relationship between ground-level PM_{2.5} concentrations and the AOD values. As the residuals represent the difference between the observed and estimated ground-level PM_{2.5} concentrations, and given that the maximum observed ground-level PM_{2.5} concentration was as large as 600 $\mu\text{g}/\text{m}^3$, the approximately -30–30 $\mu\text{g}/\text{m}^3$ range of the residuals also indicates a good agreement between the observed and estimated ground-level PM_{2.5} concentrations.

3.4. Model validation results

A regression was performed (Fig. 7) to fit the observed and estimated ground-level PM_{2.5} concentrations. The R², MPE, and RMSE were calculated (Fig. 7) to evaluate the predictive power of the time fixed effects regression model and the combined model. Subgraph (a) shows that the R² for the time fixed effects regression model was 0.71463, which was relatively high. Moreover, the R² climbed to 0.88301 after application of the GWR model, as shown in subgraph (b). At the same time, the MPE and RMSE decreased by 6.332 $\mu\text{g}/\text{m}^3$ and 7.3332 $\mu\text{g}/\text{m}^3$, respectively. This phenomenon implies that after adding the GWR model into the analysis process, the spatially heterogeneous PM_{2.5}-AOD relationship had been captured, and as a result, the accuracy of the combined model was improved. However, when we compared subgraphs (a) and (c), we found that model over-fitting was present, that is, in the

**Fig. 5.** The spatial distribution of AOD coefficients in the GWR model.**Fig. 6.** The residuals at each monitoring site and the Moran's I for them.

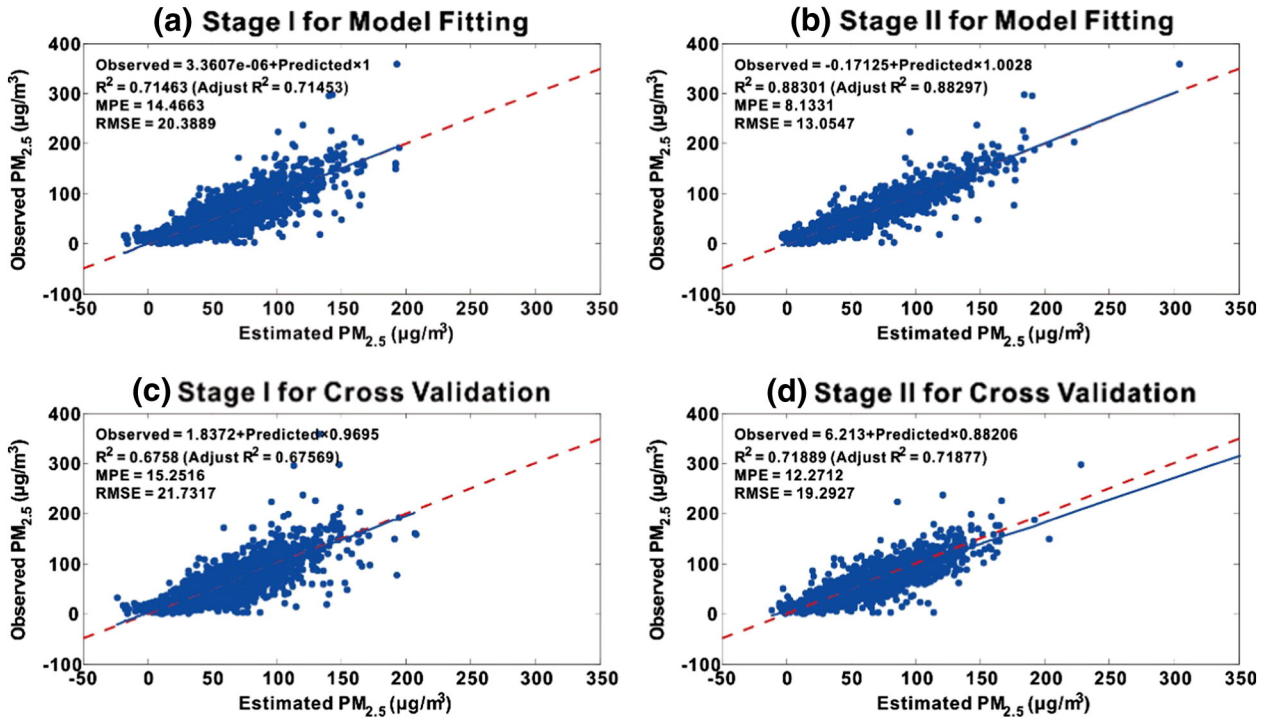


Fig. 7. Model validation.

time fixed effects regression model, from model fitting to cross validation, the R^2 had decreased by 0.03883, the MPE had increased by 0.7853 $\mu\text{g}/\text{m}^3$, and the RMSE has increased by 1.3428 $\mu\text{g}/\text{m}^3$. Unfortunately, the over-fitting became more severe after the GWR model was added. We can see that after application of the GWR model, from model fitting to cross validation, the R^2 had decreased by 0.16412, whereas the MPE and RMSE had increased by 4.1381 $\mu\text{g}/\text{m}^3$ and 6.238 $\mu\text{g}/\text{m}^3$, respectively. This small amount of over-fitting in the combined model was likely mainly due to the limited number of matched data records per day (Hu et al., 2014). Nevertheless, after the GWR model was incorporated, whether in model fitting or cross validation, from the time fixed effects regression model to the combined model, the R^2 increased and the MPE and RMSE decreased. Additionally, given that the R^2 was relatively high and the MPE and RMSE were relatively low, we can ignore this over-fitting to some extent. We also fitted the observed and estimated ground-level PM_{2.5} concentrations with the zero intercept, producing the regression equations: $\text{Estimated} = 1.0007 \times \text{Observed}$, $\text{Estimated} = 1 \times \text{Observed}$, $\text{Estimated} = 0.9931 \times \text{Observed}$, $\text{Estimated} = 0.9597 \times \text{Observed}$, corresponding to subgraphs (a)-(d), respectively. The slopes imply that in the model fitting, the estimated ground-level PM_{2.5} concentrations agreed well with the observed ground-level PM_{2.5} concentrations or just overestimated the observed ground-level PM_{2.5} concentrations to a very small extent. Moreover, in the cross validation, the estimated ground-level PM_{2.5} concentrations underestimated the observed ground-level PM_{2.5} concentrations by 1%–5%.

3.5. Prediction maps of PM_{2.5} concentrations

The estimated seasonal mean and annual mean ground-level PM_{2.5} concentrations from the time fixed effects regression model are shown in Fig. 8. They were derived from the daily results. When finished with the residual correction by using the GWR model, new seasonal and annual patterns were obtained, and these are shown in Fig. 9. From Figs. 8 and 9, which are very similar, we can roughly see the temporal and spatial variation of ground-level PM_{2.5} concentrations. More specifically,

the ground-level PM_{2.5} concentrations were high in winter and spring, low in summer, and average in autumn. Spatially, the ground-level PM_{2.5} concentrations were higher in the southeast domain and lower in the northwest domain.

To further explore the temporal and spatial variation of the ground-level PM_{2.5} concentrations, we plotted a line that passed through the center of Beijing and the center of Tianjin at the same time. We collected the concentrations along that line and plotted the results in line charts (Fig. 10), which is referred to hereafter as the cross-section analysis. Subgraphs (a) and (b) obviously revealed the temporal and spatial variation of the ground-level PM_{2.5} concentrations. First, with an increase in distance from the starting point, the concentrations showed a rising trend, and this reflects the spatial variation. Second, along the sides of the center of Beijing, approximately in the 108 km range, temporal variation was apparent; the line for spring was above the line of autumn, the line for autumn was above the line for summer, and the line for winter was not continuous because of missing data. Subgraph (c) shows the difference between subgraphs (b) and (a) (i.e., values of (b) minus those of (a)). These results show that in Beijing and Tianjin, the difference between the time fixed effects regression model and the combined model was somewhat large, especially in winter and spring, which suggests that the GWR model was necessary and meaningful. Thus, it is worthwhile to use the GWR model to capture the spatial variations, especially during heavy pollution seasons and in heavily polluted regions so as to improve the predictive power of the combined model.

In order to see the differences among all prefecture-level cities in Beijing–Tianjin–Hebei, we calculated the mean value of the ground-level PM_{2.5} concentrations in every city by using the combined model results. In particular, we presented the annual mean results in descending order and plotted a radar chart of the results, which is shown in Fig. 11. The top three cities for PM_{2.5} concentrations were Handan, Xingtai, and Shijiazhuang, which are in the southern domain of the Hebei province. Those areas are plain areas, and a number of industries occupy a great deal of land in this region; thus, industrial emissions were likely the main reason for the high ground-level PM_{2.5} concentrations. The lowest three cities for PM_{2.5} concentrations were Qinhuangdao,

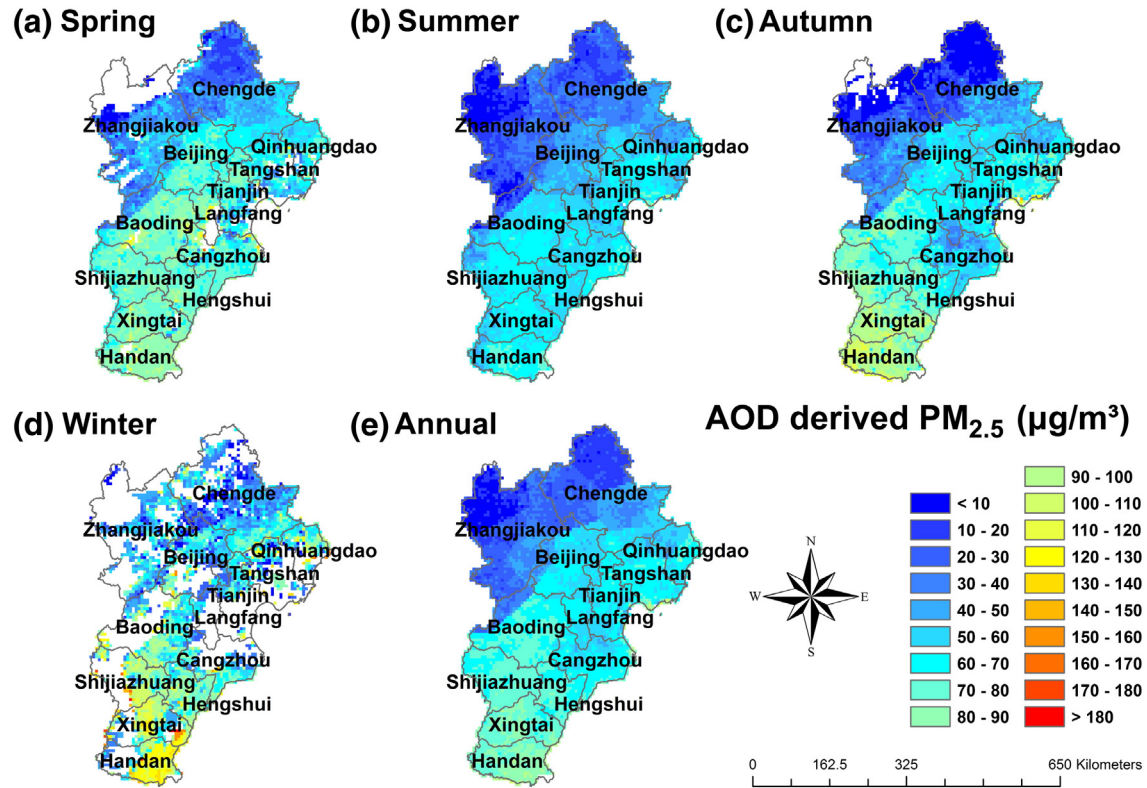


Fig. 8. Prediction maps of PM_{2.5} concentrations from the time fixed effects regression model.

Chengde, and Zhangjiakou. Those areas are mountainous areas with high levels of vegetation cover, which likely helped to suppress the ground-level PM_{2.5} concentrations. Beijing and Tianjin are municipalities in China. Moreover, Beijing is the capital of China. The air quality

in Beijing and Tianjin is concerning to many people of diverse backgrounds. Fortunately, according to our results, the ground-level PM_{2.5} concentrations in Beijing and Tianjin were relatively low compared to the whole Beijing-Tianjin-Hebei region; these areas ranked 9 out of

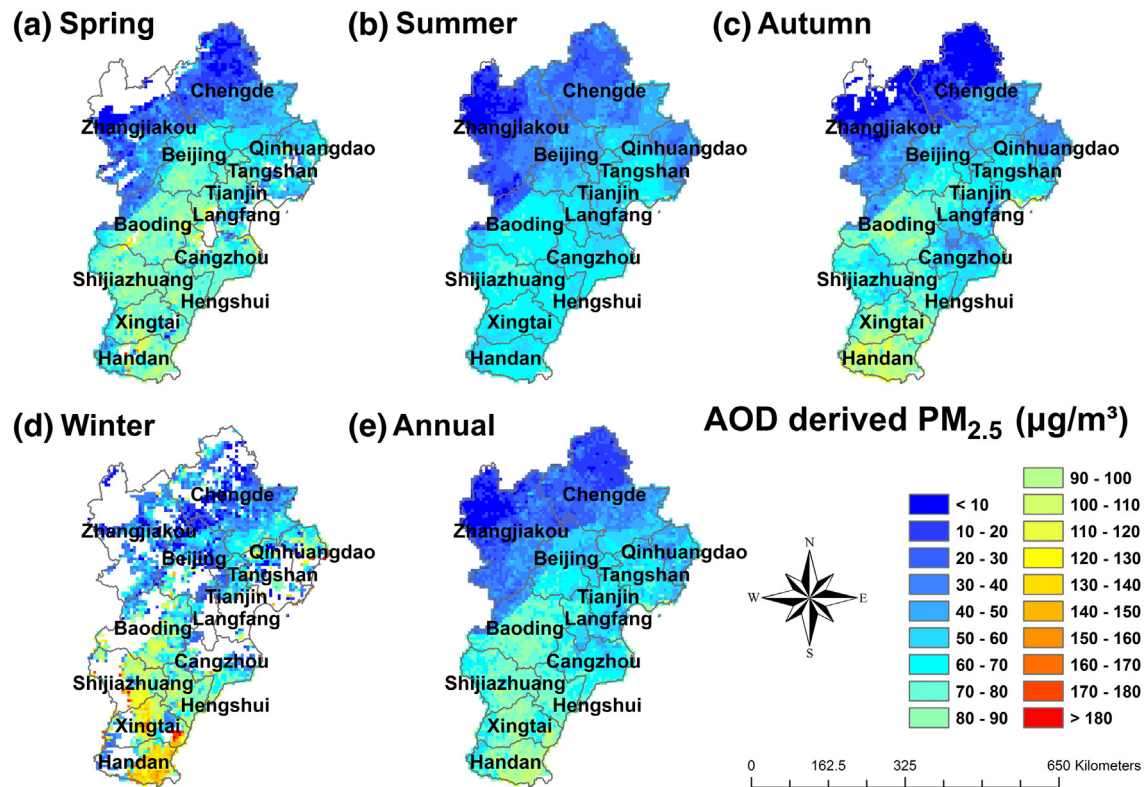


Fig. 9. Prediction maps of PM_{2.5} concentrations from the combined model.

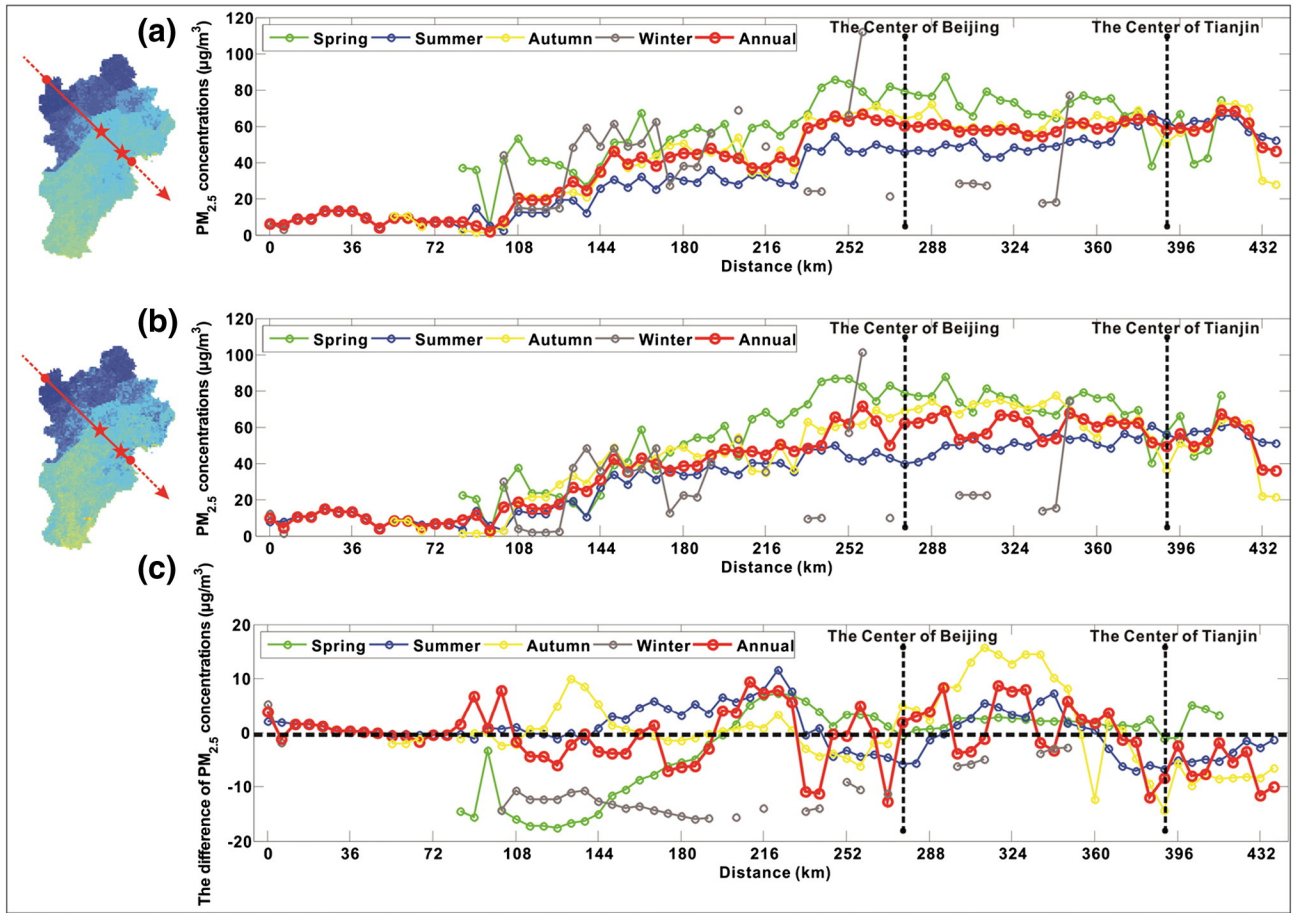


Fig. 10. Line charts of the ground-level PM_{2.5} concentrations from the cross-section analysis. (a)–(c) charts correspond to the time fixed effects regression model, the combined model, and the difference between them, respectively.

13 and 8 out of 13, respectively, which represents a medium-low level. We think that government pollution control measures being carried out in Beijing and Tianjin are the main reason for this relatively medium-low level of PM_{2.5} pollution. For example, in recent years, Beijing has successively launched policies that have been helpful for air quality improvements, such as relocating industries out of the area.

4. Discussion

In this study, we used the new VIIRS AOD retrievals as the main predictive variable to estimate ground-level PM_{2.5} concentrations in the Beijing–Tianjin–Hebei region of China. To our knowledge, this is one

of the earliest empirical studies that examine the remote sensing retrievals of ground-level PM_{2.5} concentrations from VIIRS in China. The VIIRS AOD retrievals have a higher spatial resolution compared to the conventionally used MODIS or MISR AOD retrievals. Our results indicate that the differences of the PM_{2.5} concentration patterns among different cities can be detected through the use of the new VIIRS AOD retrievals. Therefore, VIIRS AOD retrievals are suitable for estimating the regional PM_{2.5} pollution pattern.

Some new variables were also used to further improve the accuracy of the combined model, and these variables included the NO₂_Lag and four directional wind vectors. We found that without the NO₂_Lag and by using the original wind speed in the time fixed effects regression model, the model's R² was 0.6985. After changing the wind speed to the new four directional wind vectors, the model's R² became 0.7002. Finally, by employing both the NO₂_Lag and four directional wind vectors at the same time, the model's R² became 0.7146, and that was the first-stage model that we applied to further analyses in this study—the time fixed effects regression model. From 0.6895 to 0.7146, the R² had increased by approximately 2.3%. This increase was significant and illustrates the advantages of using the NO₂_Lag and four directional wind vectors in the model. We also tried employing the averaged PM_{2.5} concentrations between 13:00 pm to 14:00 pm as the dependent variable, which correspond to the Suomi-NPP satellite time of 13:30 pm, to determine if the model's performance could be improved. However, the result showed that such an approach was not worthwhile as the R² in the time fixed effects regression model only reached 0.6894. As most of the variables that we ended up using were daily averages, it remains a possibility that using the satellite transited PM_{2.5} concentrations as the dependent variable cannot improve the model's performance.

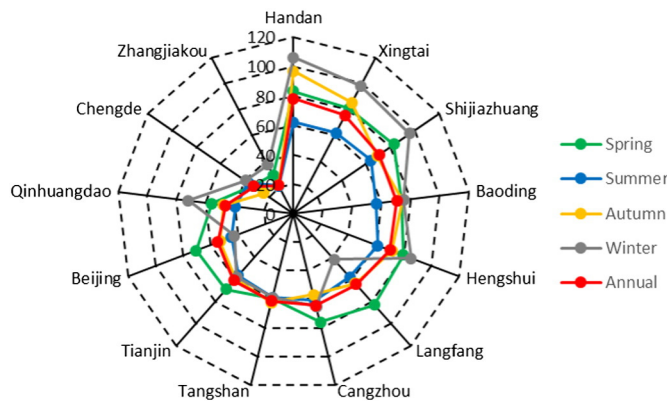


Fig. 11. Radar chart of the mean ground-level PM_{2.5} concentrations in each city.

As for the method, we used a spatiotemporal statistical model because it is expected to capture the temporal and spatial variations of PM_{2.5} concentrations simultaneously through the use of the time fixed effects regression model and GWR model. The results showed that this approach does work. Among all published papers relevant to this study, we found that efforts to simultaneously capture the temporal and spatial variations of PM_{2.5} concentrations were limited. Liu et al. (2009) used a generalized additive model to do this, Hu et al. (2014) and Ma et al. (2016) also used a two-stage model to do this. One important difference between our work and the work of Hu et al. and Ma et al. was in the first stage. We employed the time fixed effects regression model which is frequently used in panel data analysis. Hu et al. and Ma et al. employed the linear mixed effects model which is widely used for the analysis of hierarchical data and allows to accommodate complicated hierarchical correlations of observations. Practically, it is computationally lighter and operationally easier for model calibration and prediction by using our specification. Anyhow, using the time fixed effects regression model brought a comparable or even better model performance (i.e., R²) and thus we finally employed it.

As for the spatial pattern of PM_{2.5} concentrations, we found only one publication in the same period on global scale from the study of van Donkelaar et al. (2016). They have always shared their global estimated PM_{2.5} concentrations on the Dalhousie University Atmospheric Composition Analysis Group Web site (http://fizz.phys.dal.ca/~atmos/martin/?page_id=140) for free. We replotted their annual result in Beijing–Tianjin–Hebei and ours based on the same color scale and found two areas presenting significantly different characteristics (SI, Fig. S2). More specifically, our result presented lower PM_{2.5} concentrations in Beijing–Tianjin belt and higher PM_{2.5} concentrations in southwest part of the study area, indicating a wider range of PM_{2.5} concentrations. Therefore, our work has the ability to provide much more fine spatial details on fine particle pollution in Beijing–Tianjin–Hebei. It is not only because of the 6 km × 6 km spatial resolution VIIRS AOD using but also due to the spatiotemporal statistical model we developed.

In terms of the application of our work, it mainly focuses on the prediction of PM_{2.5} concentrations. Spatially, we obtained a full spatial coverage of PM_{2.5} concentrations, producing compensation for the deficiency of ground monitoring. The study area of our work was Beijing–Tianjin–Hebei region which has the characteristic of urban-industrial conditions. Even Hebei province, a region with many rural administrative units, is also covered with plenty of factories. Therefore, we believe that the principle contribution to AOD comes from the particles at the near surface level and thus the satellite linkage with the ground in Beijing–Tianjin–Hebei region can be guaranteed. Our work is a demonstration of the method and can be extended to other regions but cautions should be paid on whether the region has the characteristic of urban-industrial conditions. Temporally, we could estimate PM_{2.5} concentrations of the past and near future if we assume that the spatiotemporal variations of PM_{2.5}–AOD relationship was constant in each year, which needs more evidences and we will collect more data to analyze it in the near future. The full spatiotemporal covered estimation of PM_{2.5} concentrations from our study is certain to be helpful for epidemiologic studies and pollution control policy making in Beijing–Tianjin–Hebei.

There are some limitations associated with our work that should be discussed. The first limitation is the deficiency of matched data records per day. We had to use the averaged values in the GWR model so as to avoid obtaining no solution with the GWR equations for some days. We may solve this problem through seeking a trade-off between the minimum number of matched data records per day and the model overfitting degree for studies in the near future. The discovery strategy may be set up as follows. As Hu et al. (2014) pointed out, the overfitting degree of a two-stage model incorporating GWR can be reduced when the number of matched data records per day increases. Therefore, we want to explore the relationship between them and hope to find out an optimal threshold of the minimum number of matched data records

per day. First, we can define the difference between R² during model fitting and cross validation as the model's overfitting degree. As the minimum number of matched data records per day increases, a lower model overfitting degree appears and the days which cannot meet the condition are removed. Then we can create a line chart taking the cumulative losing days as the x-axis and the corresponding model overfitting degree as the y-axis. We may find an inflection point in that line, before which the model's overfitting degree decreases rapidly and after which the model's overfitting degree decreases slowly. The number of matched data records per day corresponding to that inflection point is the optimal threshold we would accept. Finally, we can get the maximum reduction of the model's overfitting degree at the minimum days lost price with that threshold. Another limitation is that the data integration method is relatively simple. We plan on using more rigorous scientific data integration methods in the near future, such as by adopting the mean value of some variables over a certain range from the monitoring site, which can be realized through buffer analysis, and by adopting spline interpolation for the meteorological data instead of nearest neighbor interpolation (Thiessen polygons), which has been proven less accurate for meteorological data compared with the former.

5. Conclusions

This study aimed to develop a spatiotemporal statistical model to estimate ground-level PM_{2.5} concentrations. In contrast to most existing research, we used the VIIRS AOD retrievals as the main predictive independent variable and incorporated some new independent variables to further improve the combined model's performance. The results were satisfactory, though some limitations still exist; we hope to work on these issues in the future. Here, we list the major conclusions of this study.

- i. Fine particulate pollution in the Beijing–Tianjin–Hebei region is severe, and the annual PM_{2.5} concentration was found to be 92.3 µg/m³.
- ii. Compared with the traditional ordinary least squares method, the time fixed effects regression model performed much better, and it was able to capture the temporal variation of the PM_{2.5}–AOD relationships.
- iii. Residual spatial autocorrelation was encountered when the time fixed effects regression model was used alone, but after applying the GWR model, the residual spatial autocorrelation was alleviated, thus indicating that the GWR model can capture the spatial variation of the PM_{2.5}–AOD relationships.
- iv. The ground-level PM_{2.5} concentrations were significantly affected by meteorological factors, land use characteristics, and other variables. Specifically, temperature, SRH, and the NO₂_Lag had positive relationships with the ground-level PM_{2.5} concentrations, whereas rainfall, PBLH, RH_PBLH, the four directional wind vectors, and NDVI had negative relationships with the ground-level PM_{2.5} concentrations.
- v. By applying the combined model, we were able to produce fine particle pollution maps for the Beijing–Tianjin–Hebei region. The temporal and spatial variations of the concentrations were obvious. Seasonally, the concentrations were higher in winter and spring, lower in summer, and moderate in autumn. Spatially, the concentrations were higher in the southeast domain, which includes Handan, Xingtai, and Shijiazhuang, and they were lower in the northwest domain, which includes Zhangjiakou and Chengde.

Acknowledgements

This study was financially supported by the National Natural Science Foundation of China (No. 41471370). We thank anonymous reviewers and the editor for their constructive comments.

Appendix A. Supplementary data

Supplementary data to this article can be found online at <http://dx.doi.org/10.1016/j.rse.2016.07.015>.

References

- Abernethy, R.C., Allen, R.W., McKendry, I.G., Brauer, M., 2013. A land use regression model for ultrafine particles in Vancouver, Canada. *Environ. Sci. Technol.* 47, 5217–5225.
- Amini, H., Taghavi-Shahri, S.M., Henderson, S.B., Naddafi, K., Nabizadeh, R., Yunesian, M., 2014. Land use regression models to estimate the annual and seasonal spatial variability of sulfur dioxide and particulate matter in Tehran, Iran. *Sci. Total Environ.* 488, 343–353.
- Boersma, K.F., Eskes, H.J., Dirksen, R.J., van der A, R.J., Veefkind, J.P., Stammes, P., Huijnen, V., Kleipool, Q.L., Sneep, M., Claas, J., Leitao, J., Richter, A., Zhou, Y., Brunner, D., 2011. An improved tropospheric NO₂ column retrieval algorithm for the ozone monitoring instrument. *Atmos. Meas. Tech.* 4, 1905–1928.
- Brunsdon, C., Fotheringham, A.S., Charlton, M.E., 1996. Geographically weighted regression: a method for exploring spatial nonstationarity. *Geogr. Anal.* 28, 281–298.
- Cheng, Y., He, K.B., Du, Z.Y., Zheng, M., Duan, F.K., Ma, Y.L., 2015. Humidity plays an important role in the PM2.5 pollution in Beijing. *Environ. Pollut.* 197, 68–75.
- Dominici, F., Peng, R.D., Bell, M.L., Pham, L., McDermott, A., Zeger, S.L., Samet, J.M., 2006. Fine particulate air pollution and hospital admission for cardiovascular and respiratory diseases. *JAMA*, *J. Am. Med. Assoc.* 295, 1127–1134.
- Engel-Cox, J.A., Holloman, C.H., Coutant, B.W., Hoff, R.M., 2004. Qualitative and quantitative evaluation of MODIS satellite sensor data for regional and urban scale air quality. *Atmos. Environ.* 38, 2495–2509.
- Fotheringham, A.S., Charlton, M., Brunsdon, C., 1996. The geography of parameter space: an investigation of spatial non-stationarity. *Int. J. Geogr. Inf. Syst.* 10, 605–627.
- Fotheringham, A., Brusdon, C., Charlton, M., 2002. Geographically Weighted Regression: The Analysis of Spatially Varying Relationships. John Wiley & Sons Inc.
- Henderson, S.B., Beckerman, B., Jerrett, M., Brauer, M., 2007. Application of land use regression to estimate long-term concentrations of traffic-related nitrogen oxides and fine particulate matter. *Environ. Sci. Technol.* 41, 2422–2428.
- HJ618–2011, 2011. Determination of atmospheric articles PM10 and PM2.5 in ambient air by gravimetric method. Available at http://english.mep.gov.cn/standards_reports/.
- Hoff, R.M., Christopher, S.A., 2009. Remote sensing of particulate pollution from space: Have We reached the promised land? *J. Air Waste Manage. Assoc.* 59, 645–675.
- Hu, X.F., Waller, L.A., Al-Hamdan, M.Z., Crosson, W.L., Estes, M.G., Estes, S.M., Quattrochi, D.A., Sarnat, J.A., Liu, Y., 2013. Estimating ground-level PM2.5 concentrations in the southeastern US using geographically weighted regression. *Environ. Res.* 121, 1–10.
- Hu, X.F., Waller, L.A., Lyapustin, A., Wang, Y.J., Al-Hamdan, M.Z., Crosson, W.L., Estes, M.G., Estes, S.M., Quattrochi, D.A., Puttaswamy, S.J., Liu, Y., 2014. Estimating ground-level PM2.5 concentrations in the Southeastern United States using MAIAC AOD retrievals and a two-stage model. *Remote Sens. Environ.* 140, 220–232.
- Jackson, J.M., Liu, H.Q., Laszlo, I., Kondragunta, S., Remer, L.A., Huang, J.F., Huang, H.C., 2013. Suomi-NPP VIIRS aerosol algorithms and data products. *J. Geophys. Res. Atmos.* 118, 12673–12689.
- Jia, S.L., Su, L., Tao, J.H., Wang, Z.F., Chen, L.F., Shang, H.Z., 2014. A study of multiple regression method for estimating concentration of fine particulate matter using satellite remote sensing. *China Environ. Sci.* 34 (3), 565–573 (in Chinese).
- Li, C.C., Mao, J.T., Liu, Q.H., Yuan, Z.B., Wang, M.H., Liu, X.Y., 2005. The application of remote sensing aerosol products from MODIS data in the research on air pollution of Beijing. *Sci. China Ser. D Earth Sci.* 35 (Suppl. I), 177–186 (in Chinese).
- Li, R., Gong, J.H., Chen, L.F., Wang, Z.F., 2015. Estimating ground-level PM2.5 using fine-resolution satellite data in the megacity of Beijing, China. *Aerosol Air Qual. Res.* 15, 1347–1356.
- Liu, A.X., Han, S.Q., Yao, Q., Zhang, M., Cai, Z.Y., 2013. Characteristics of chemical composition of PM2.5 and its effect on visibility in autumn and winter of 2011 in Tianjin. *J. Meteorol. Environ.* 29 (2), 42–47 (in Chinese).
- Liu, Y., Sarnat, J.A., Kilaru, A., Jacob, D.J., Koutrakis, P., 2005. Estimating ground-level PM2.5 in the eastern United States using satellite remote sensing. *Environ. Sci. Technol.* 39, 3269–3278.
- Liu, Y., Franklin, M., Kahn, R., Koutrakis, P., 2007. Using aerosol optical thickness to predict ground-level PM2.5 concentrations in the St. Louis area: a comparison between MISR and MODIS. *Remote Sens. Environ.* 107, 33–44.
- Liu, Y., Paciorek, C.J., Koutrakis, P., 2009. Estimating regional spatial and temporal variability of PM2.5 concentrations using satellite data, meteorology, and land use information. *Environ. Health Perspect.* 117, 886–892.
- Ma, Z.W., Hu, X.F., Huang, L., Bi, J., Liu, Y., 2014. Estimating ground-level PM2.5 in China using satellite remote sensing. *Environ. Sci. Technol.* 48, 7436–7444.
- Ma, Z., Hu, X., Sayer, A.M., Levy, R., Zhang, Q., Xue, Y., Tong, S., Bi, J., Huang, L., Liu, Y., 2016. Satellite-based spatiotemporal trends in PM2.5 concentrations: China, 2004–2013. *Environ. Health Perspect.* 124, 184–192.
- Ministry of Environmental Protection of the People's Republic of China, 2012l. Ambient air quality standards (GB3095–2012). http://kjs.mep.gov.cn/hjbhbz/bzw/bdqhjzbz/dqhzlbz/201203/20120302_224165.htm.
- Ministry of Environmental Protection of the People's Republic of China, 2013l. Under the state council concerning the action plan for the control of air pollution [EB/OL]. –09–12[2011–09–12] http://zfs.mep.gov.cn/fg/gwyw/201309/t20130912_260045.htm.
- Nowak, D.J., Crane, D.E., Stevens, J.C., 2006. Air pollution removal by urban trees and shrubs in the United States. *Urban For. Urban Green.* 4 (3), 115–123.
- Pope, C.A., Dockery, D.W., 2006. Health effects of fine particulate air pollution: lines that connect. *J. Air Waste Manage. Assoc.* 56, 709–742.
- Pope, C.A., Burnett, R.T., Thun, M.J., Calle, E.E., Krewski, D., Ito, K., Thurston, G.D., 2002. Lung cancer, cardiopulmonary mortality, and long-term exposure to fine particulate air pollution. *JAMA*, *J. Am. Med. Assoc.* 287, 1132–1141.
- Pugh, T.A.M., MacKenzie, A.R., Whyatt, J.D., Hewitt, C.N., 2012. Effectiveness of green infrastructure for improvement of air quality in urban street canyons. *Environ. Sci. Technol.* 46, 7692–7699.
- Rienecker, M.M., Suarez, M.J., Gelaro, R., Todling, R., Bacmeister, J., Liu, E., Bosilovich, M.G., Schubert, S.D., Takacs, L., Kim, G.K., Bloom, S., Chen, J.Y., Collins, D., Conaty, A., Da Silva, A., Gu, W., Joiner, J., Koster, R.D., Lucchesi, R., Molod, A., Owens, T., Pawson, S., Pegion, P., Redder, C.R., Reichle, R., Robertson, F.R., Ruddick, A.G., Sienkiewicz, M., Woollen, J., 2011. MERRA: NASA's modern-era retrospective analysis for research and applications. *J. Clim.* 24, 3624–3648.
- Schliep, E.M., Gelfand, A.E., Holland, D.M., 2015. Autoregressive spatially varying coefficients model for predicting daily PM_{2.5} using VIIRS satellite AOT. *Adv. Stat. Climatol. Meteorol. Oceanogr.* 1, 59–74.
- Schueler, C., Clement, J.E., Ardanuy, P., Welsch, C., DeLucia, F., Swenson, H., 2002. NPOESS VIIRS Sensor Design Overview. In: Barnes, W.L. (Ed.), *Earth Observing Systems VI*. SPIE-Int Soc Optical Engineering, Bellingham, pp. 11–23.
- Song, W.Z., Jia, H.F., Huang, J.F., Zhang, Y.Y., 2014. A satellite-based geographically weighted regression model for regional PM2.5 estimation over the Pearl River Delta region in China. *Remote Sens. Environ.* 154, 1–7.
- Tan, W.Z., 2007. The Basic Theoretics and Application Research on Geographically Weighted Regression. Tongji University, Shanghai.
- Tao, J., Xie, W.Z., Xu, Z.C., Peng, X.C., 2007. Analysis on variation trends of atmospheric visibility and its effect factors in winter in Guangzhou. *Urban Environ. Urban Ecol.* 2007 (1), 17–20 (in Chinese).
- van Donkelaar, A., Martin, R.V., Brauer, M., Kahn, R., Levy, R., Verdúzco, C., Villeneuve, P.J., 2010. Global estimates of ambient fine particulate matter concentrations from satellite-based aerosol optical depth: development and application. *Environ. Health Perspect.* 118, 847–855.
- van Donkelaar, A., Martin, R.V., Brauer, M., Boys, B.L., 2015. Use of satellite observations for long-term exposure assessment of global concentrations of fine particulate matter. *Environ. Health Perspect.* 123, 135–143.
- van Donkelaar, A., Martin, R.V., Brauer, M., Hsu, N.C., Kahn, R.A., Levy, R.C., Lyapustin, A., Sayer, A.M., Winker, D.M., 2016. Global estimates of fine particulate matter using a combined geophysical-statistical method with information from satellites, models, and monitors. *Environ. Sci. Technol.* 50, 3762–3772.
- Wang, J., Aegeerter, C., Xu, X., Szykman, J.J., 2016. Potential application of VIIRS day/night band for monitoring nighttime surface PM_{2.5} air quality from space. *Atmos. Environ.* 124, 55–63.
- Wu, J.S., Li, J.C., Peng, J., Li, W.F., Xu, G., Dong, C.C., 2015. Applying land use regression model to estimate spatial variation of PM2.5 in Beijing, China. *Environ. Sci. Pollut. Res.* 22, 7045–7061.
- Zhang, Y.L., Cao, F., 2015. Fine Particulate Matter (PM2.5) in China at a City Level. *Sci. Rep.* 5, 14884.
- Zhu, G.R., Guo, L.Z., Yin, G.B., Xu, Y.L., 2010. Map Design and Compilation. 2re ed. Wuhan University Press, Wuhan, p. 98.